

Specific Absorption Rate and Temperature Increase in Human Eye Subjected to Electromagnetic Fields at 900 MHz

Teerapot Wessapan

Phadungsak Rattanadecho¹

e-mail: ratphadu@engr.tu.ac.th

Research Center of Microwave Utilization
in Engineering (R.C.M.E.),
Department of Mechanical Engineering,
Faculty of Engineering,
Thammasat University,
Rangsit Campus,
Pathumthani 12120, Thailand

Human eye is one of the most sensitive parts of the entire human body when exposed to electromagnetic fields. These electromagnetic fields interact with the human eye and may lead to cause a variety of ocular effects from high intensity radiation. However, the resulting thermo-physiologic response of the human eye to electromagnetic fields is not well understood. In order to gain insight into the phenomena occurring within the human eye with temperature distribution induced by electromagnetic fields, a detailed knowledge of absorbed power distribution as well as temperature distribution is necessary. This study presents a numerical analysis of specific absorption rate (SAR) and heat transfer in the heterogeneous human eye model exposed to electromagnetic fields. In the heterogeneous human eye model, the effect of power density on specific absorption rate and temperature distribution within the human eye is systematically investigated. In particular, the results calculated from a developed heat transfer model, considered natural convection and porous media theory, are compared with the results obtained from a conventional heat transfer model (based on conduction heat transfer). In all cases, the temperatures obtained from the developed heat transfer model have a lower temperature gradient than that of the conventional heat transfer model. The specific absorption rate and the temperature distribution in various parts of the human eye during exposure to electromagnetic fields at 900 MHz, obtained by numerical solution of electromagnetic wave propagation and heat transfer equation, are also presented. The results show that the developed heat transfer model, which is the more accurate way to determine the temperature increase in the human eye due to electromagnetic energy absorption from electromagnetic field exposure. [DOI: 10.1115/1.4006243]

Keywords: electromagnetic fields, temperature distribution, specific absorption rate, human eye, heat transfer

1 Introduction

In the recent years, there is an increasing public concern about the interaction between the human body and electromagnetic fields. It is well known that the human eye is one of the most sensitive parts of the entire human body that can exhibit thermal damage due to electromagnetic fields exposure. Therefore, it is interesting to investigate on the possible ocular effects occurred during exposure to electromagnetic fields. Although the safety standards are regulated in terms of the peak SAR value of tissue, the maximum temperature increase in the human eye caused by electromagnetic energy absorption is an actual influence of the dominant factors, which induce adverse physiological effects. The severity of the physiological effect produced by small temperature increases can cause eyesight to worsen. There have been medical case reports of the formation of cataracts in humans following the accidental exposure to microwave radiation [1]. Actually, a small temperature increase in the eye of 3–5 °C leads to induce cataracts formation [2]. Additionally, it is reported that a temperature above 41 °C is necessary for production of posterior lens opacities [3]. Numerical analysis of human eye exposed to electromagnetic fields has provided useful information on absorption of

electromagnetic energy for the human eye under a variety of exposure condition.

In the past, there have been reports on the effects of electromagnetic fields on the human eye [4,5]. Nevertheless, the analysis generally has been conducted based on peak SAR, which follows public safety standards regulation [6,7]. The experimental data on the correlation of SAR levels to the temperature increases in human tissue are still sparse. Most previous studies of human exposed to electromagnetic fields have not been considered the heat transfer causing an incomplete analysis to the results. Therefore, modeling of heat transport in human tissues is needed to cooperate with the modeling of electromagnetic in order to completely explain these interaction characteristics for approaching realistic phenomena.

The topic of temperature increase in human tissue caused by exposure to electromagnetic fields, particularly those radiated to the eye, has been of interest for several years. Recently, the modeling of heat transport in human tissue has been investigated by many researchers [8–20]. Thermal modeling of human tissue is important as a tool to investigate the effect of external heat sources as well as in predicting the abnormalities within the tissue. In the past, most studies of heat transfer analysis in human eye used heat conduction equation [8–14]. Some studies carried out on natural convection in human eye based on heat conduction model [15,16]. Ooi and Ng [16] studied the effect of aqueous humor (AH) hydrodynamics on the heat transfer within the eye based on heat conduction model. Meanwhile, the bioheat equation, introduced by Pennes [17,18]

¹Corresponding author.

Contributed by the Heat Transfer Division of ASME for publication in the JOURNAL OF HEAT TRANSFER. Manuscript received July 28, 2011; final manuscript received February 14, 2012; published online July 9, 2012. Assoc. Editor: Pamela M. Norris.

based on the heat diffusion equation for a blood perfused tissue, is used for modeling of heat transfer in the human eye as well [19,20]. Recently, porous media models have been utilized to investigate the transport phenomena in biological media instead simplified bioheat model [21–23]. Shafahi and Vafai [24] proposed the porous media along with natural convection model to analyze the eye thermal characteristics during exposure to thermal disturbances. The other research groups have been tried to conduct the advanced model using the coupled model of heat and electromagnetic dissipation in the human eye [10–14].

Our research group has tried to numerically investigate the temperature increase in the human tissues subjected to electromagnetic fields in many problems [25–27]. Wessapan et al. [25,26] utilized a 2D finite element method (FEM) to obtain the SAR and temperature increase in human body exposed to leakage electromagnetic wave. Wessapan et al. [27] developed a three-dimensional human head model in order to investigate the SAR and temperature distribution in human head during exposure to mobile phone radiation. Keangin et al. [28,29] carried out on the numerical simulation of liver cancer treated using the complete mathematical model considered the coupled model of electromagnetic wave propagation, heat transfer, and mechanical deformation in biological tissue in the couple way.

Most previous studies of the interaction between electromagnetic field and the human eye were mainly focused on SAR and have not been considered heat transfer causing an incomplete analysis to the results. Therefore, modeling of heat transport is needed in order to completely explain the actual process of interaction between electromagnetic field and the human eye within the human tissue. Although porous media and natural convection models of human eye have been used in the previous biomedical studies [15,16,24], most studies of human eye exposed to electromagnetic fields have not been considering the porous media approach, and natural convection approach is sparse or nonexistent.

There are few studies on the temperature and electromagnetic field interaction in realistic physical model of the human organs especially human eye due to the complexity of the problem, even though it is directly related to the thermal injury of tissues. Therefore, in order to provide information on levels of exposure and health effects from electromagnetic field exposure adequately, it is essential to simulate both of electromagnetic field and heat transfer based on porous media theory within an anatomically model particularly human eye.

This study presents the simulation of the SAR distribution and temperature distribution in an anatomically human eye exposed to electromagnetic field based on porous media theory. This is a pioneer work in the application of natural convection and porous media theory to the study of the interaction between electromagnetic field and the human eye. In this study, a two-dimensional human eye model was used to simulate the SAR and temperature distribution in the human eye model. Electromagnetic wave propagation in the human eye was investigated by using Maxwell's equations. An analysis of heat transfer in the human eye exposed to TM-mode of electromagnetic fields was investigated using a developed heat transfer model (included the conduction and natural convection heat transfer mode) which proposed by Shafahi and Vafai [24]. In the heterogeneous human eye model, the effect of power density on specific absorption rate and temperature distribution within the human eye is systematically investigated. In particular, the results obtained from a developed heat transfer model, considered natural convection and porous media theory, are compared with the results obtained from a conventional heat transfer model (heat conduction model). The specific absorption rate and the temperature distribution in various parts of the human eye during exposure to electromagnetic fields at 900 MHz, which are obtained by numerical solution of electromagnetic wave propagation and heat transfer equation, are presented. The obtained values represent the accurate phenomena to determine the temperature increase in the human eye due to electromagnetic energy absorption from electromagnetic field exposure.

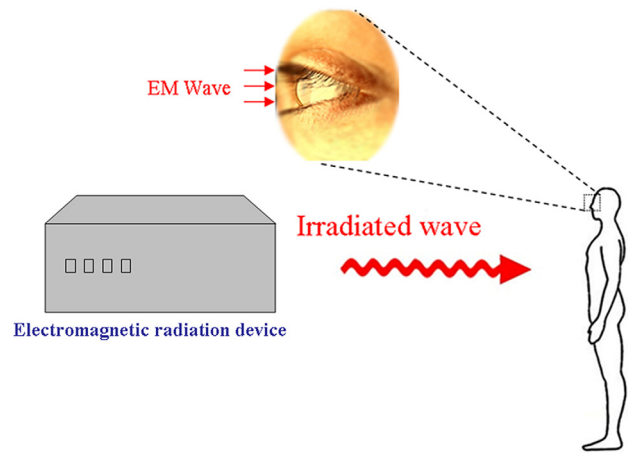


Fig. 1 Electromagnetic fields from an electromagnetic radiation device

2 Formulation of the Problem

Figure 1 shows radiation of electromagnetic fields from an electromagnetic radiation device to the human body. These electromagnetic fields fall on the human eye that causes heating in the deeper tissue, which leads to tissue damage and cataract formation. Due to ethical consideration, exposing a human to electromagnetic fields for the experimental purposes is limited. It is more convenient to develop a realistic human eye model through numerical simulation. In Sec. 3, an analysis of specific absorption rate and heat transfer in the human eye exposed to electromagnetic fields will be illustrated. The system of governing equations as well as initial and boundary conditions are solved numerically using the FEM via COMSOLTMMULTIPHYSICS.

3 Methods and Model

The first step in evaluating the effects of a certain exposure to electromagnetic fields in the human eye is the determination of the induced internal electromagnetic field and its spatial distribution. Thereafter, electromagnetic energy absorption which results in temperature increases within the human eye and other interactions will be able to be considered.

3.1 Physical Model. In this study, a two-dimensional model of the human eye, which follows the physical model in the previous research [24], is developed. Figure 2 shows the

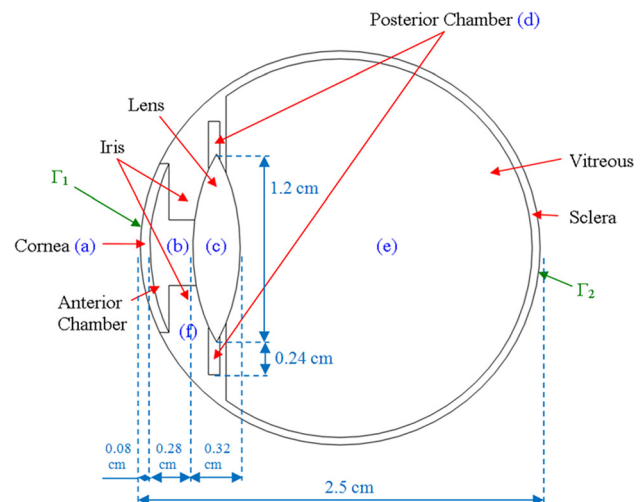


Fig. 2 Human eye vertical cross section

Table 1 Dielectric properties of tissues at 900 MHz [30,31]

Tissue	Frequency: 900 MHz	
	ϵ_r	σ (S/m)
Cornea (a)	52.0	1.85
Anterior chamber (b)	73.0	1.97
Lens (c)	51.3	0.89
Posterior chamber (d)	73.0	1.97
Vitreous (e)	74.3	1.97
Sclera (f)	52.1	1.22
Iris (f)	52.1	1.22

two-dimensional human eye model used in this study. This model comprises seven types of tissue including cornea, anterior chamber, posterior chamber, iris, sclera, lens, and vitreous. These tissues have different dielectric and thermal properties. In the sclera layer, there are two more layers known as the choroid and retina, which are relatively thin compared with the sclera. To simplify the problem, these layers are assumed to be homogeneous. The iris and sclera, which have the same properties, are modeled together as one homogenous region [16]. The dielectric properties and thermal properties of tissues are given in Tables 1 and 2, respectively. Each tissue is assumed to be homogeneous and electrically as well as thermally isotropic.

3.2 Equations for Electromagnetic Wave Propagation Analysis. Mathematical models are developed to predict the electric field and SAR with relation to temperature gradient within the human eye. To simplify the problem, the following assumptions are made:

- (1) Electromagnetic wave propagation is modeled in two dimensions.
- (2) The human eye in which electromagnetic waves interact with human eye proceeds in the open region.
- (3) The free space is truncated by scattering boundary condition.
- (4) The model assumes that dielectric properties of each tissue are constant.
- (5) In the human eye, an electromagnetic wave is characterized by transverse magnetic fields (TM-Mode).

The electromagnetic wave propagation in human eye is calculated using Maxwell's equations which mathematically describe the interdependence of the electromagnetic waves. The general form of Maxwell's equations is simplified to demonstrate the electromagnetic field penetrated in human eye as the following equation:

$$\nabla \times \left(\left(\epsilon_r - \frac{j\sigma}{\omega\epsilon_0} \right)^{-1} \nabla \times H_z \right) - \mu_r k_0^2 H_z = 0 \quad (1)$$

where H is the magnetic field (A/m), μ_r is the relative magnetic permeability, ϵ_r is the relative dielectric constant, $\epsilon_0 = 8.8542 \times 10^{-12}$ F/m is the permittivity of free space, and k_0 is the free space wave number (m^{-1}).

3.2.1 Boundary Condition for Wave Propagation Analysis. Electromagnetic energy is emitted by an electromagnetic radiation device and falls on the human eye with a particular power density. Therefore, boundary condition for solving electromagnetic wave propagation, as shown in Fig. 3, is described as follows.

Table 2 Thermal properties of human eyes [16]

Tissue	ρ (kg/m ³)	k (W/m ² C)	C_p (J/kg°C)	μ (N s/m ²)	β (1/K)
Cornea (a)	1050	0.58	4178	—	—
Anterior chamber (b)	996	0.58	3997	0.00074	0.000337
Lens (c)	1000	0.4	3000	—	—
Posterior chamber (d)	996	0.58	3997	—	—
Vitreous (e)	1100	0.603	4178	—	—
Sclera (f)	1050	1.0042	3180	—	—
Iris (f)	1050	1.0042	3180	—	—

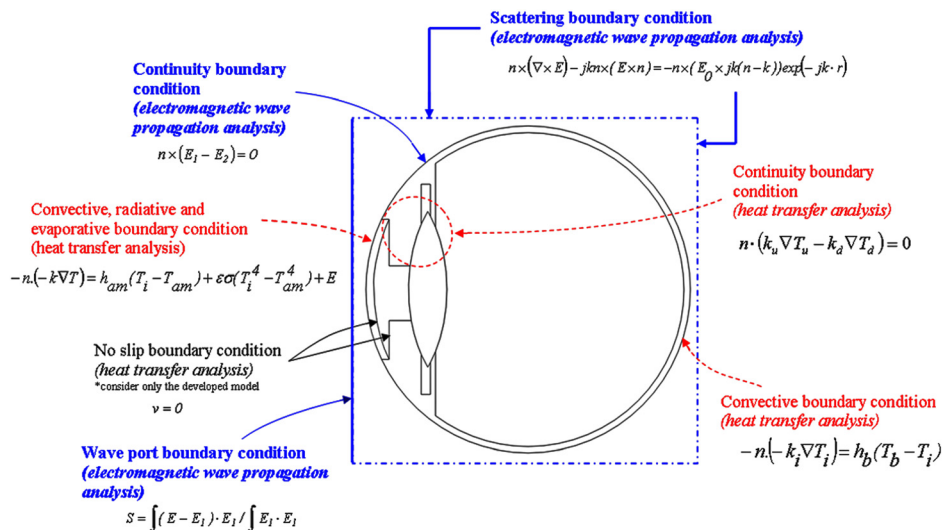


Fig. 3 Boundary condition for analysis of electromagnetic wave propagation and heat transfer

It is assumed that the uniform wave flux falls on the left side of the human eye. Therefore, at the left boundary of the considered domain, an electromagnetic simulator employs TM wave propagation port with specified power density

$$S = \int (E - E_1) \cdot E_1 / \int E_1 \cdot E_1 \quad (2)$$

Boundary conditions along the interfaces between different mediums, for example, between air and tissue or tissue and tissue, are considered as continuity boundary condition

$$n \times (E_1 - E_2) = 0 \quad (3)$$

The outer sides of the calculated domain, i.e., free space, are considered as scattering boundary condition [25]

$$n \times (\nabla \times E_z) - jkE_z = -jk(1 - k \cdot n)E_{0z} \exp(-jk \cdot r) \quad (4)$$

where k is the wave number (m^{-1}), σ is electric conductivity (S/m), n is normal vector, $j = \sqrt{-1}$, and E_0 is the incident plane wave (V/m).

3.3 Interaction of Electromagnetic Fields and Human Tissues. Interaction of electromagnetic fields with biological tissues can be defined in term of SAR. When electromagnetic waves propagate through the human tissues, the energy of electromagnetic waves is absorbed by the tissues. The specific absorption rate is defined as power dissipation rate normalized by material density [25]. The specific absorption rate is given by

$$SAR = \frac{\sigma}{\rho} |E|^2 \quad (5)$$

where E is the electric field intensity (V/m), σ is the electric conductivity (S/m), and ρ is the tissue density (kg/m^3).

3.4 Equations for Heat Transfer Analysis. To solve the thermal problem, the coupled effects of electromagnetic wave propagation and unsteady bioheat transfer are investigated. The temperature distribution is corresponded to the SAR. This is because the specific absorption rate within the human eye distributes owing to energy absorption. Thereafter, the absorbed energy is converted to thermal energy, which increases the tissue temperature.

Heat transfer analysis of the human eye is modeled in two dimensions. To simplify the problem, the following assumptions are made:

- (1) Human tissues are biomaterial with constant thermal properties.
- (2) There is no phase change of substance within the tissues.
- (3) There is local thermal equilibrium between the blood and tissue.
- (4) There is no chemical reaction within the tissues.

This study utilized two pertinent thermal models to investigate the heat transfer behavior of the human eye when exposed to the electromagnetic fields.

Model I: The conventional heat transfer model [20].

This model assumes metabolic heat generation and blood perfusion in the human eye to be zero. The governing equation solved, therefore, resembled the classical heat conduction equation

$$\rho_i C_i \frac{\partial T_i}{\partial t} = \nabla \cdot (k_i \nabla T_i) + Q_{\text{ext}}; \quad i = a, b, c, d, e, f \quad (6)$$

where i denotes each subdomain in human eye model as shown in Fig. 2, ρ is the tissue density (kg/m^3), C is the heat capacity of tissue (J/kg K), k is the thermal conductivity of

tissue (W/m K), T is the tissue temperature (K), and t is the time, respectively.

Model II: The developed heat transfer model [24].

In this model, the motion of fluid is only considered inside the anterior chamber [16]. There is blood flow in the iris/sclera part, which plays a role to adjust eye temperature with the rest of the body [24]. For the rest parts, the metabolic heat generation is neglected based on the fact that these comprise mainly water [16]. The equation governing the flow of heat in cornea, posterior chamber, lens, and vitreous is the same as that given in Eq. (6).

This model accounts for the existence of AH in the anterior chamber. The heat transfer process consists of both conduction and natural convection, which can be written as follows:

$$\text{Continuity equation: } \nabla \cdot u_i = 0; \quad i = b \quad (7)$$

Momentum equation:

$$\rho_i \frac{\partial v_i}{\partial t} + \rho_i u_i \nabla \cdot u_i = -\nabla p_i + \nabla \cdot [\mu(\nabla u_i + \nabla u_i^T)] + \rho_i g \beta_i (T_i - T_{\text{ref}}); \quad i = b \quad (8)$$

where β is the volume expansion coefficient (1/K), u is the velocity (m/s), p is the pressure (N/m²), μ is the dynamic viscosity of AH (N s/m²), and T_{ref} is the reference temperature which we have considered here is 37 °C. The effects of buoyancy due to the temperature gradient are modeled using the Boussinesq approximation which states that the density of a given fluid changes slightly with temperature but negligibly with pressure [16].

Energy equation:

$$\rho_i C_i \frac{\partial T_i}{\partial t} - \nabla \cdot (k_i \nabla T_i) = -\rho C_i v_i \cdot \nabla T_i + Q_{\text{ext}}; \quad i = b \quad (9)$$

The sclera/iris is modeled as a porous medium with blood perfusion, which assumes local thermal equilibrium between the blood and tissue. The blood perfusion rate used is 0.004 1/s. A modified Pennes' bioheat equation [24,32] is used to calculate the temperature distribution within the sclera/iris.

$$(1 - \varepsilon) \rho_i C_i \frac{\partial T_i}{\partial t} = \nabla \cdot ((1 - \varepsilon) k_i \nabla T_i) + \rho_b C_b \omega_b (T_b - T_i) + Q_{\text{ext}}; \quad i = f \quad (10)$$

where T_b is the temperature of blood (K), ρ_b is the density of blood (kg/m^3), C_b is the specific heat capacity of blood (J/kg K), ω_b is the blood perfusion rate (1/s), and Q_{ext} is the external heat source term (electromagnetic heat source density) (W/m³).

In the analysis, the porosity (ε) used is assumed to be 0.6. The heat conduction between tissue and blood flow is approximated by the blood perfusion term, $\rho_b C_b \omega_b (T_b - T)$.

The external heat source term is equal to the resistive heat generated by electromagnetic field (electromagnetic power absorbed), which defined as [25]

$$Q_{\text{ext}} = \frac{1}{2} \sigma_{\text{tissue}} |\bar{E}|^2 = \frac{\rho}{2} \cdot SAR \quad (11)$$

where σ_{tissue} is the electric conductivity of tissue (S/m).

3.4.1 Boundary Condition for Heat Transfer Analysis. The heat transfer analysis, which does not include parts of the surrounding space, is considered only in the human eye. As shown in Fig. 3, the cornea surface is considered as the convective, radiative, and evaporative boundary condition for all of the models

$$-n \cdot (-k \nabla T) = h_{\text{am}} (T_i - T_{\text{am}}) + \varepsilon \sigma (T_i^4 - T_{\text{am}}^4) + e \quad \text{on } \Gamma_1 \quad i = a \quad (12)$$

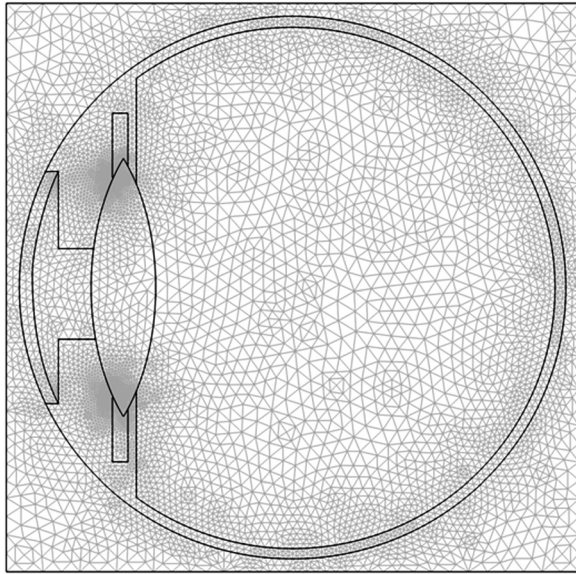


Fig. 4 A two-dimensional finite element mesh of human eye model

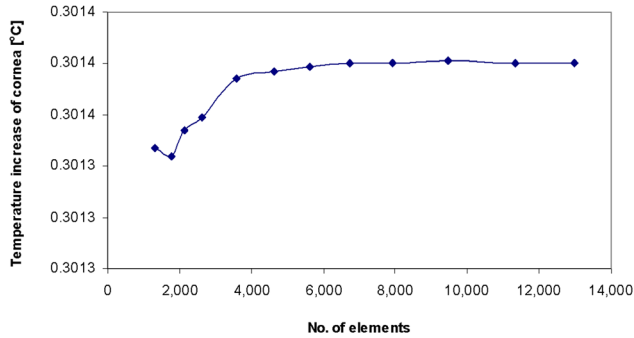


Fig. 5 Grid convergence curve of the 2D model

where Γ_i is the external surface area corresponding to section i , e is the tear evaporation heat loss (W/m^2), T_{am} is the ambient temperature (K), and h_{am} is convection coefficient ($\text{W}/\text{m}^2 \text{K}$).

The temperature of blood which is generally assumed to be the same as the body core temperature causes heat to be transferred into the eye [16]. The surface of the sclera is assumed to be a convective boundary condition for all of the models

$$-n \cdot (-k_i \nabla T_i) = h_b (T_b - T_i) \quad \text{on } \Gamma_2 \quad i = f \quad (13)$$

where h_b is convection coefficient of blood ($65 \text{ W}/\text{m}^2 \text{K}$). Γ_1 and Γ_2 are corneal surface and sclera surface of the eye, respectively.

3.5 Calculation Procedure. In this study, the finite element method is used to analyze the transient problems. The computational scheme is to assemble finite element model and compute a local heat generation term by performing an electromagnetic calculation using tissue properties. In order to obtain a good approximation, a fine mesh is specified in the sensitive areas. This study provides a variable mesh method for solving the problem as shown in Fig. 4. The system of governing equations as well as initial and boundary conditions are then solved. All computational processes are implemented using COMSOLTM MULTIPHYSICS, to demonstrate the phenomenon that occurs within the human eye exposed to electromagnetic fields.

The 2D model is discretized using triangular elements and the Lagrange quadratic is then used to approximate temperature and

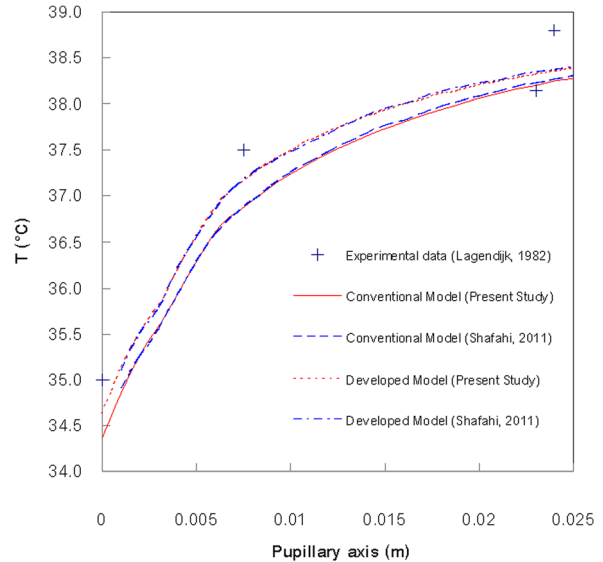


Fig. 6 Comparison of the calculated temperature distribution to the temperature distribution obtained by Shafahi and Vafai, and the Legendijk's experimental data; $h_{\text{am}} = 20 \text{ W}/\text{m}^2 \text{K}$ and $T_{\text{am}} = 25^\circ \text{C}$

SAR variation across each element. Convergence test is carried out to identify the suitable number of elements required. The convergence curve resulting from the convergence test is shown in Fig. 5. This convergence test leads to the grid with approximately 10,000 elements. It is reasonable to assume that, at this element number, the accuracy of the simulation results is independent from the number of elements.

4 Results and Discussion

In this study, the coupled model of electromagnetic field and thermal field are solved numerically. For the simulation, the dielectric properties and thermal properties are directly taken from Tables 1 and 2, respectively. The exposed radiated power used in this study refers to ICNIRP standard for safety level at the maximum SAR value of $2 \text{ W}/\text{kg}$ (general public exposure) and $10 \text{ W}/\text{kg}$ (occupational exposure) [6]. For the electromagnetic frequency of 900 MHz, the effect of power density on distributions of specific absorption rate and temperature profile within the human eye is systematically investigated using two models, namely, the conventional heat transfer model (models I) and the developed heat transfer model (model II).

4.1 Verification of the Model. In order to verify the accuracy of the present numerical models, the case without electromagnetic field of the simulated results from the present study is validated against the numerical results with the same geometric model obtained by Shafahi and Vafai [24]. Moreover, the numerical results are then compared with the experimental results of the rabbit obtained from Legendijk [8]. The validation case assumes that the rabbit body temperature is 38.8°C , the tear evaporation heat loss is $40 \text{ W}/\text{m}^2$, the ambient temperature is 25°C , and convection coefficient of ambient air is $20 \text{ W}/\text{m}^2 \text{K}$. The results of the selected test case are illustrated in Fig. 6 for temperature distribution in the eyes. Figure 6 clearly shows a good agreement of the temperature distribution in the eye between the present solution and that of Shafahi and Vafai [24] and Legendijk [8]. In the figure, the simulated results of the conventional heat transfer model (models I) and the developed heat transfer model (model II) provide a good agreement with the simulated results obtained from Shafahi and Vafai [24]. This favorable comparison lends confidence in the accuracy of the present numerical model.

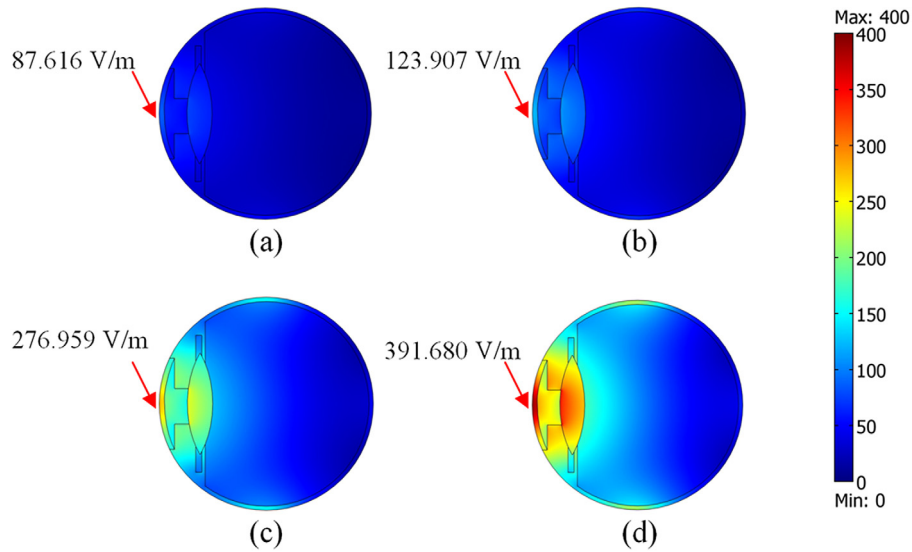


Fig. 7 Electric field distribution (V/m) in human eye exposed to the electromagnetic frequency of 900 MHz at the power densities of (a) 5 mW/cm², (b) 10 mW/cm², (c) 50 mW/cm², and (d) 100 mW/cm²

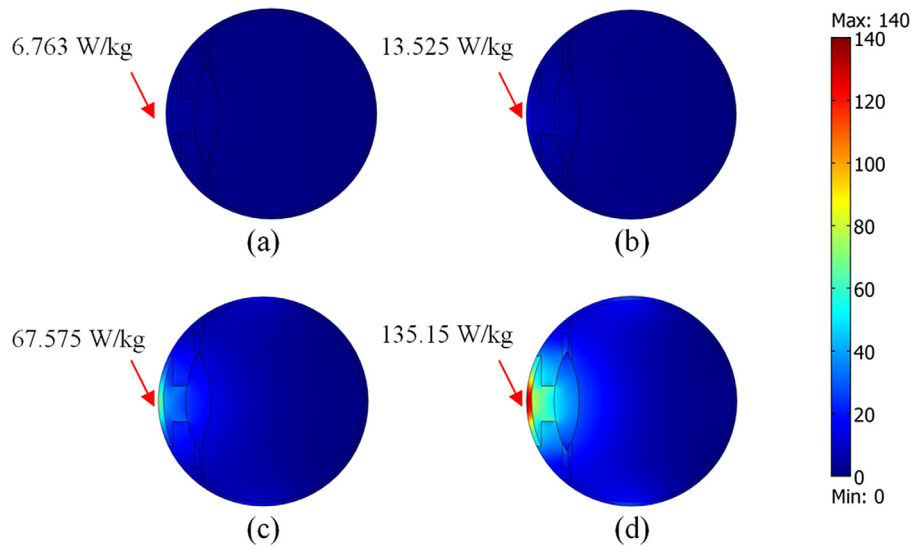


Fig. 8 SAR distribution (W/kg) in human eye exposed to the electromagnetic frequency of 900 MHz at the power densities of (a) 5 mW/cm², (b) 10 mW/cm², (c) 50 mW/cm², and (d) 100 mW/cm²

4.2 Electric Field Distribution. To illustrate the penetrated electric field distribution inside the human eye, the predicted results obtained from our proposed models are required. Figure 7 shows the simulation of electric field pattern inside the human eye exposed to electromagnetic field in TM mode operating at the frequency of 900 MHz propagating along the vertical cross section human eye model where the varying power densities are done. Due to the different dielectric characteristics of the various tissue layers, a different fraction of the supplied electromagnetic energy will become absorbed in each layer in the human eye. Consequently, the reflection and transmission components at each layer contribute to the resonance of standing wave in the human eye. It can be seen that the higher values of electric field in all cases occur in the outer part area of the eye, especially in cornea, and lens. Certainly, the maximum electric field intensity at the higher power density is greater than that of the lower power density. The maximum electric field intensities are 391.680 V/m, 276.959 V/m,

123.907 V/m, and 87.616 V/m at the power densities of 100 mW/cm², 50 mW/cm², 10 mW/cm², and 5 mW/cm², respectively. The three highest electric field intensity values in the human eye at all power densities occur in cornea, lens, and iris, respectively. This is because the lower value of their dielectric properties (ϵ_r) shown in Table 1 which corresponds to Eq. (1), as well as these tissues located close to the exposed surface, by which it causes the electromagnetic field can penetrate easily into these tissues. The electric field deep inside the human eye is extinguished where the electric field attenuates due to absorbed electromagnetic energy and is then converted to heat. Moreover, the electric field distribution also showed a strong dependence on the dielectric properties of the tissues.

4.3 SAR Distribution. Figure 8 shows the SAR distribution evaluated on the vertical cross section of the human eye exposed

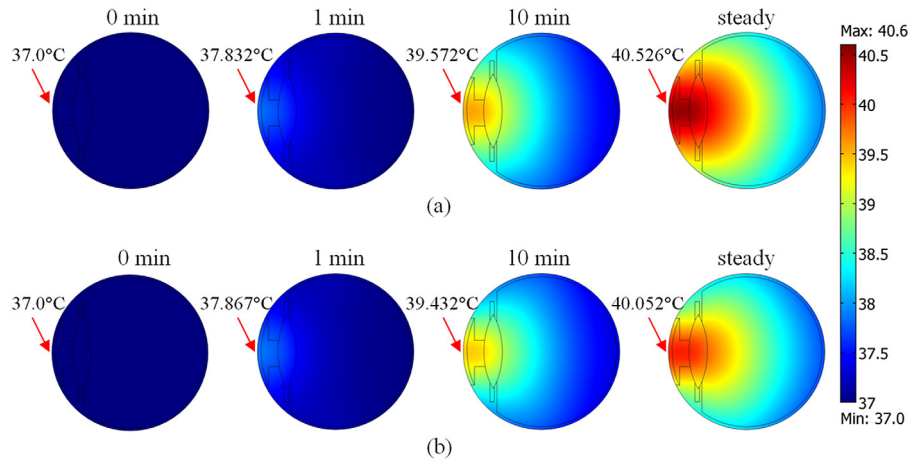


Fig. 9 The temperature distribution in human eye at various time exposed to the electromagnetic frequency of 900 MHz at the power density of 100 mW/cm^2 calculated using (a) the conventional heat transfer model (b) the developed heat transfer model

to the electromagnetic frequency of 900 MHz at various power densities. It is evident from the figure that the results of the SAR values within the human eye (Fig. 8) which are increased corresponding to the electric field intensities (Fig. 7). Besides the electric field intensity, the magnitude of dielectric properties and thermal properties in each tissue will directly affect the amount of SAR within the human eye. For all power densities, the highest SAR values are obtained only in the region of the cornea but not in lens and iris as electric field distributions. This is because the cornea has a much higher value of its dielectric properties (σ) than those of the lens and iris, as well as the cornea located close to the exposed surface, at which the electric field intensity is strongest. It is found that the SAR distribution pattern in the human eye, which corresponds to Eq. (5), is strongly depended on the effect of the dielectric properties (σ , shown in Table 1) and thermal properties (ρ , shown in Table 2). With penetration into the eye, the SAR values decrease rapidly along the distance from the electromagnetic source. The maximum SAR values are 135.15 W/kg , 67.575 W/kg , 13.525 W/kg , and 6.763 W/kg at the power densities of 100 mW/cm^2 , 50 mW/cm^2 , 10 mW/cm^2 , and 5 mW/cm^2 , respectively. Comparing to ICNIRP standard for safety level at the maximum SAR value of 2 W/kg (general public exposure) and 10 W/kg (occupational exposure) [6], the resulting SAR values from this study are higher than the ICNIRP exposure limits for occupational exposure in most cases except for the power density of 5 mW/cm^2 .

4.4 Temperature Distribution. Since this study has focused on the volumetric heating effect into the multilayered eye induced by electromagnetic field, the effect of ambient temperature variation have been neglected in order to gain insight into the interaction between electromagnetic field and human tissues as well as the correlation between SAR and heat transfer mechanism. For this reason, the ambient temperature has been set to human body temperature of 37°C , and the tear evaporation has been neglected. Moreover, the effect of thermoregulation mechanisms has also been neglected due to the small temperature increase occurred during exposure process. The convective coefficient due to blood flow inside the sclera is set to $65 \text{ W/m}^2 \text{ K}$ [16]. In order to study the heat transfer within the human eye, the coupled effects of electromagnetic wave propagation and unsteady heat transfer as well as initial and boundary conditions are then investigated. Due to these coupled effects, the electric field distribution in Fig. 7 and the SAR distribution in Fig. 8 are then converted into heat by absorption of the tissues. Figure 9 shows the temperature distribution in the vertical cross section human eye at various time

exposed to the electromagnetic frequency of 900 MHz at the power density of 100 mW/cm^2 calculated using the conventional heat transfer model (model I) (Fig. 9(a)) and developed heat transfer model (model II) (Fig. 9(b)). For the human eye exposed to the electromagnetic fields for a period of time, the temperature within the human eye (Fig. 9) is increased corresponding to the specific absorption rate (Fig. 8). This is because the electric field within the human eye attenuates owing to the energy absorbed and thereafter the absorbed energy is converted to thermal energy, which increases the human eye temperature.

It is found that by using the different heat transfer models, the distribution patterns of temperature at a particular time are quite different. The hot spot zone is strongly displayed at the 10 min for the both heat transfer models at the anterior chamber area, owing to the extensive penetration of electromagnetic power of internal regions and higher dielectric properties (ϵ_r) of anterior chamber tissue. This higher dielectric property of the anterior chamber represents the stronger absorption ability of electromagnetic fields than those of the cornea and lens. The outer corneal surface has a lower temperature than that of the anterior chamber, even if it has higher SAR value (Fig. 8). This is because heat is dissipated to the ambient via convection and radiation. Since the main heat transfer mechanism of the conventional heat transfer model is thermal conduction of the human eye, whereas the developed heat transfer model accounts for the natural convection within the anterior chamber as well. Therefore, the developed heat transfer model with higher dissipation rates of heat generated by electromagnetic fields can obtain higher cooling effect than that of the conventional heat transfer model.

Consider the temperature increase distribution at the extrusion line (Fig. 10). Figure 11 shows the temperature increase versus papillary axis (along the extrusion line) of human eye exposed to the electromagnetic frequency of 900 MHz at various times. In the early stage of exposure (1 min), the calculated temperature in the anterior chamber, obtained from the conventional heat transfer model, is little lower than that of developed heat transfer model. This is because natural convection in the developed heat transfer model causes a substantial accumulation of warmer fluid in the upper half of the anterior chamber. Surprisingly, just after 10 min of exposure, the temperature increase of the conventional heat transfer model is higher than that of developed heat transfer model. This is due to the presence of blood perfusion in the iris/sclera tissues, which covers an internal surface area of the human eye. This blood perfusion provides buffer characteristic to the human eye temperature, which is expected to occur in the realistic physiological conditions. Moreover, the natural convection and formation of two circulatory patterns with opposite direction

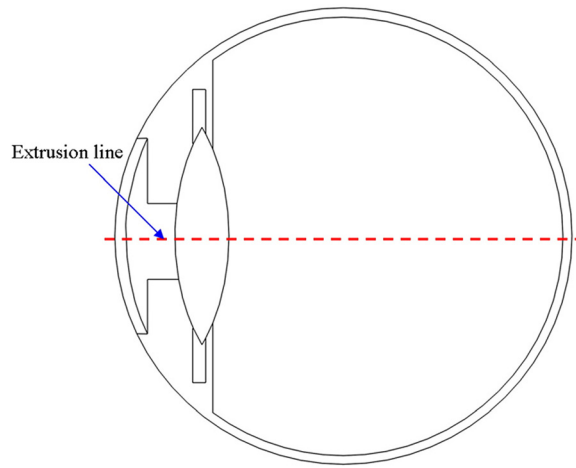


Fig. 10 The extrusion line in the human eye where the temperature distribution is considered

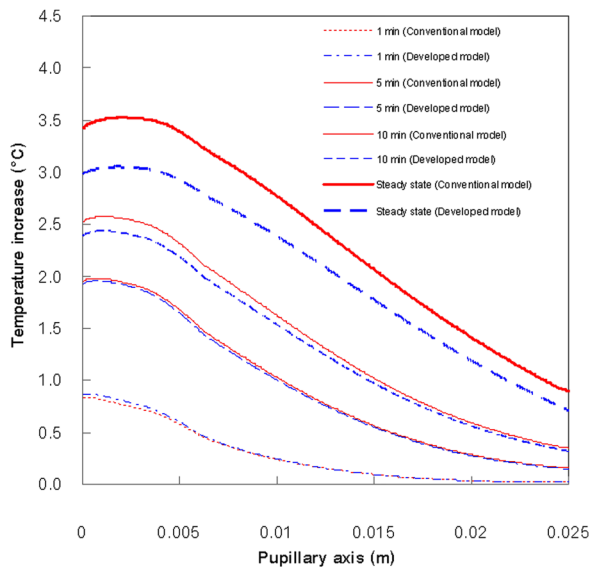


Fig. 11 Temperature increase versus pupillary axis of human eye exposed to the electromagnetic frequency of 900 MHz at various times

within the anterior chamber, shown in Fig. 12, play important roles on the cooling processes in the human eye, especially inner corneal surface, when a large temperature gradient is produced by electromagnetic fields after 10 min. The circulation pattern implies that the generated heat in the anterior chamber is convected in two directions; one is to the corneal surface, and the other to the lens surface. The circulation pattern in this study is quite different from that of that of the previous studies [16,24] because of the different heating pattern within the human eye. The difference is that in this study, volumetric heat source by electromagnetic fields is adopted, but in the previous studies, surface heating was imposed on the human eye.

The effect of power density (the power irradiated on the human eye surface) has also investigated. Figure 13 shows the comparison of the temperature distribution within the human eye at time approaching to steady state condition with the frequency of 900 MHz corresponding to the power densities of 5 mW/cm², 10 mW/cm², 50 mW/cm², and 100 mW/cm². It is found that the power densities significantly influence the temperature increase within the human eye. Greater power density provides greater

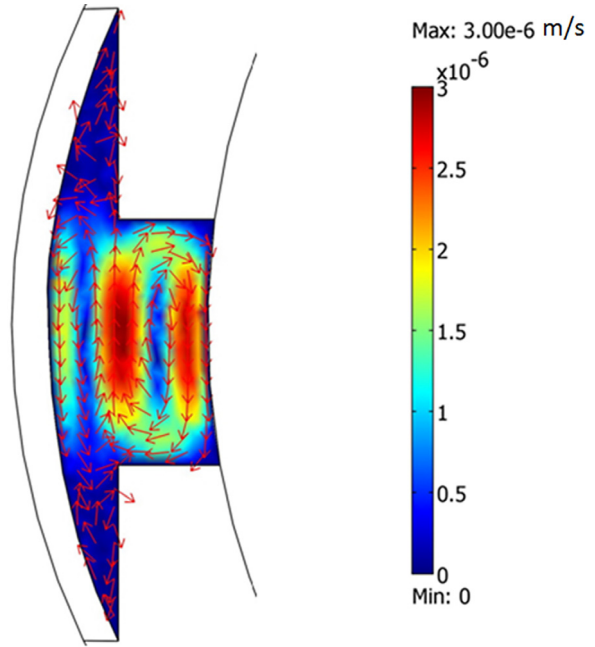


Fig. 12 The velocity distribution inside the anterior chamber in human eye when exposed to the electromagnetic frequency of 900 MHz

heat generation inside the human eye, thereby increasing the rate of temperature rise. By using the conventional heat transfer model, the maximum temperature increases are 0.177 °C, 0.353 °C, 1.764 °C, and 3.526 °C at the power densities of 5 mW/cm², 10 mW/cm², 50 mW/cm², and 100 mW/cm², respectively. By using the developed heat transfer model, the maximum temperature increases are 0.153 °C, 0.305 °C, 1.527 °C, and 3.052 °C at the power densities of 5 mW/cm², 10 mW/cm², 50 mW/cm², and 100 mW/cm², respectively. In all cases, the maximum temperature increases obtained from the developed heat transfer model have a lower temperature than that of the conventional heat transfer model. This is due to the presence of blood perfusion which provides buffer characteristic to the human eye temperature, as well as the natural convection within the anterior chamber, shown in Fig. 14, play important roles on the cooling processes in the human eye. Figure 14 shows the circulatory patterns within the anterior chamber in human eye exposed to the electromagnetic frequency of 900 MHz at various power densities. These circulatory patterns within the anterior chamber vary corresponding to the power densities which produced the temperature gradient within the human eye. Therefore, in the case of a lower power density, the circulatory patterns have a lower speed, where a circulatory pattern with a higher power density flows faster. At the lower power density with low flow speed, the heat transfer in the anterior chamber occurs mainly by conduction across the fluid layer. In the case of the higher power density with higher flow speed, different flow regimes are encountered, with a progressively increasing heat transfer. The fluid motion within the anterior chamber is driven by the power density which is associated with the Grashof number Gr . The Grashof number is defined as $Gr = g\beta q D^5 / (k\nu^2)$, in which D is the eye diameter (m), q is internal power density (W/m²), and ν is kinematic viscosity (m²/s). The range of Grashof numbers investigated is from 5.04×10^3 to 1.01×10^5 as shown in Fig. 14.

Figure 15 shows the steady state temperature increase versus pupillary axis (along the extrusion line shown in Fig. 10) of human eye exposed to the electromagnetic frequency of 900 MHz at various power densities. This figure shows that the effects of natural convection and blood perfusion in the developed heat transfer model (model II) have a substantial impact on the

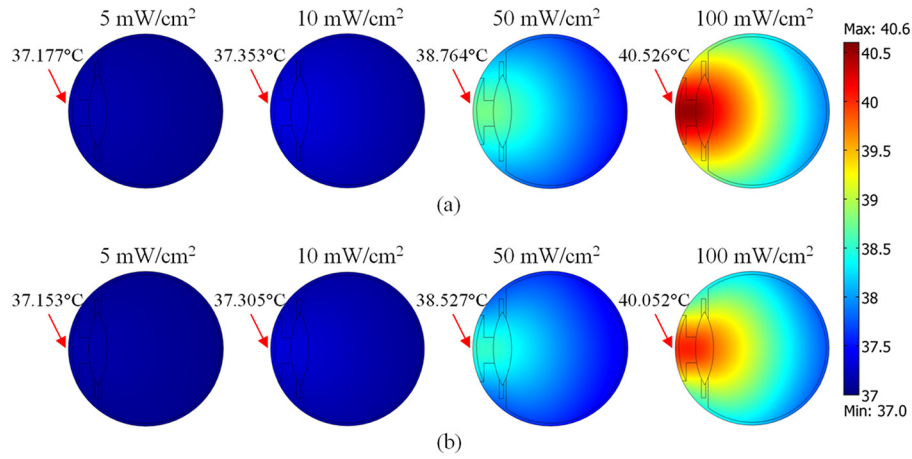


Fig. 13 The temperature distribution in human eye exposed to the electromagnetic frequency of 900 MHz at various power densities calculated using (a) the conventional heat transfer model (b) the developed heat transfer model

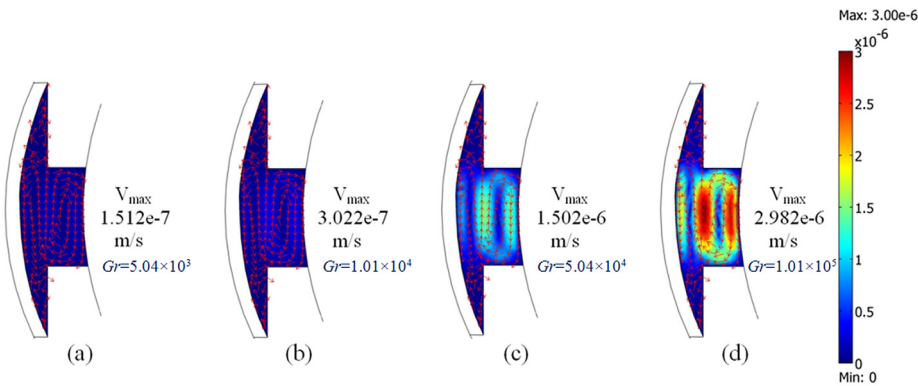


Fig. 14 The velocity distribution inside the anterior chamber in human eye exposed to the electromagnetic frequency of 900 MHz at the power densities of (a) 5 mW/cm², (b) 10 mW/cm², (c) 50 mW/cm², and (d) 100 mW/cm²

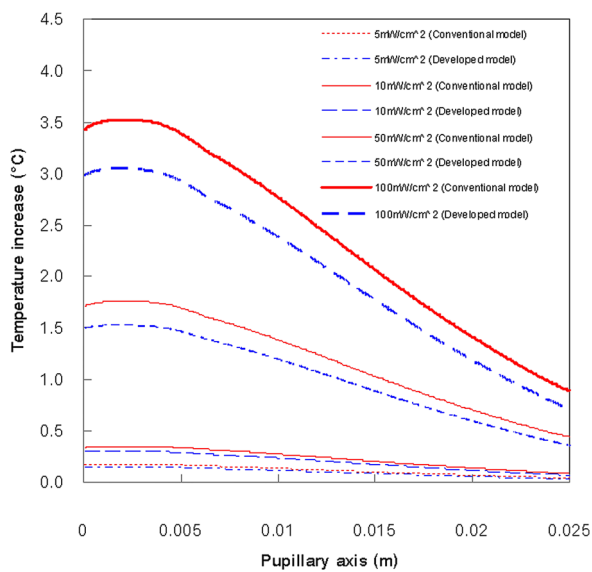


Fig. 15 Steady state temperature increases versus pupillary axis of human eye exposed to the electromagnetic frequency of 900 MHz at various power densities

calculated temperature increases in all power densities. In case of low power density, the temperature increase distribution obtained from both heat transfer models are nearly the same, which corresponds to a low temperature gradient. However, in case of higher power density, the temperature increase distribution obtained from both heat transfer models is significantly different. This is because a large temperature gradient produced by an electromagnetic field causes a strong effect of natural convection as well as the presence of blood perfusion which provides buffer characteristic to the human eye temperature.

In this study, the maximum temperature increases occur in the anterior chamber with the power density of 100 mW/cm² calculated using the conventional heat transfer model and the developed heat transfer model are 3.526 °C and 3.052 °C, respectively. The obtained temperature increases may lead to the formation of cataract or posterior capsular opacification [2].

5 Conclusions

This study presents the numerical simulation of SAR and temperature distribution in the human eye exposed to TM-mode of electromagnetic fields at 900 MHz with the power densities of 5 mW/cm², 10 mW/cm², 50 mW/cm², and 100 mW/cm². The numerical simulations in this study show several important features of the energy absorption in the human eye. Refer to SAR values, the exposed radiated power used in this study refers to ICNIRP

standard for safety level at the maximum SAR value of 2 W/kg (general public exposure) and 10 W/kg (occupational exposure) [6]. The resulting SAR from this study is exceeded the limit value for occupational exposure in most cases except for the power density of 5 mW/cm². This is because the SAR values vary corresponding to the power densities which produced the temperature increase within the human eye. Therefore, in the case of a lower power density of 5 mW/cm², the SAR value does not exceed the specified SAR limits.

In particular, the temperature results obtained from a developed heat transfer model, considered natural convection and porous media theory, are compared with the results obtained from a conventional heat transfer model in order to highlight the advantages and the weakness of each model. It is found that by using the different heat transfer models, the distribution patterns of temperature at a particular time are quite different. In all cases, the temperatures obtained from the developed heat transfer model have a lower temperature than that of the conventional heat transfer model. This is due to the presence of blood perfusion, which provides buffer characteristic to the human eye temperature, as well as the natural convection within the anterior chamber. It is found that greater power density results in a greater heat generation inside the human eye, thereby increasing the rate of temperature increase. Moreover, it is found that the temperature distributions in human eye induced by electromagnetic fields are not directly related to the SAR distribution due to the effect of dielectric properties, thermal properties, blood perfusion, and penetration depth of the electromagnetic power.

Therefore, health effect assessment of electromagnetic field exposure requires the utilization of the most accurate numerical simulation of the thermal model along with the SAR model. In the future works, the effect of ambient temperature variation will be included in the analysis to represent the actual heat transfer process which occurs in the realistic situation and will focus on the frequency-dependent dielectric properties of human tissue. A study will also be developed to a more realistic 3D model for simulations and to study the temperature dependency of dielectric property. This will allow a better understanding of the realistic situation of the interaction between electromagnetic fields and the human tissues.

Acknowledgment

This work was supported by the National Research University Project of Thailand, Office of Higher Education Commission and the Thailand Research Fund (TRF).

Nomenclatures

C = specific heat capacity (J/kg K)
 E = electric field intensity (V/m)
 e = the tear evaporation heat loss (W/m²)
 f = frequency of incident wave (Hz)
 H = magnetic field (A/m)
 h = convection coefficient (W/m² K)
 j = current density (A/m²)
 k = thermal conductivity (W/(m K))
 n = normal vector
 p = pressure (N/m²)
 Q = heat source (W/m³)
 T = temperature (K)
 u = velocity (m/s)
 t = time

Greek Letters

B = volume expansion coefficient (1/K)
 μ = magnetic permeability (H/m)
 ε = permittivity (F/m)
 σ = electric conductivity (S/m)
 ω = angular frequency (rad/s)

ρ = density (kg/m³)
 ω_b = blood perfusion rate (1/s)
 Γ = external surface area

Subscripts

am = ambient
 b = blood
 ext = external
 i = subdomain
 met = metabolic
 r = relative
 ref = reference
 0 = free space, initial condition

References

- [1] Emery, A. F., Kramar, P., Guy, A. W., and Lin, J. C., 1975, "Microwave Induced Temperature Rises in Rabbit Eyes in Cataract Research," *ASME Trans. J. Heat Transfer*, **97**, pp. 123–128.
- [2] Buccella, C., Santis, V. D., and Feliaiani, M., 2007, "Prediction of Temperature Increase in Human Eyes Due to RF Sources," *IEEE Trans. Electromagn. Compat.*, **49**(4), pp. 825–833.
- [3] Lin, J. C., 2003, "Cataracts and Cell-Phone Radiation," *IEEE Antennas Propag. Mag.*, **45**(1), pp. 171–174.
- [4] Fujiwara, O., and Kato, A., 1994, "Computation of SAR Inside Eyeball for 1.5-GHz Microwave Exposure Using Finite-Difference Time Domain Technique," *IEICE Trans.*, **E77-B**, pp. 732–737.
- [5] Gandhi, O. P., Lazzi, G., and Furse, C. M., 1996, "Electromagnetic Absorption in the Human Head and Neck for Mobile Telephones at 835 and 1900 MHz," *IEEE Trans. Microwave Theory Tech.*, **44**(10), pp. 1884–1897.
- [6] International Commission on Non-Ionizing Radiation Protection (ICNIRP), 1998, "Guidelines for Limiting Exposure to Time-Varying Electric, Magnetic and Electromagnetic Fields (Up to 300 GHz)," *Health Phys.*, **74**, pp. 494–522.
- [7] IEEE, 1999, "IEEE Standard for Safety Levels With Respect to Human Exposure to Radio Frequency Electromagnetic Fields, 3 kHz to 300 GHz," IEEE Standard, C95.1–1999.
- [8] Legendijk, J. J. W., 1982, "A Mathematical Model to Calculate Temperature Distribution in Human and Rabbit Eye During Hyperthermic Treatment," *Phys. Med. Biol.*, **27**, pp. 1301–1311.
- [9] Scott, J., 1988, "A Finite Element Model of Heat Transport in the Human Eye," *Phys. Med. Biol.*, **33**, pp. 227–241.
- [10] Scott, J., 1988, "The Computation of Temperature Rises in the Human Eye Induced by Infrared Radiation," *Phys. Med. Biol.*, **33**, pp. 243–257.
- [11] Amara, E. H., 1995, "Numerical Investigations on Thermal Effects of Laser–Ocular Media Interaction," *Int. J. Heat Mass Transfer*, **38**, pp. 2479–2488.
- [12] Hirata, A., Matsuyama, S., and Shiozawa, T., 2000, "Temperature Rises in the Human Eye Exposed to EM Waves in the Frequency Range 0.6–6 GHz," *IEEE Trans. Electromagn. Compat.*, **42**(4), pp. 386–393.
- [13] Chua, K. J., Ho, J. C., Chou, S. K., and Islam, M. R., 2005, "On the Study of the Temperature Distribution Within a Human Eye Subjected to a Laser Source," *Int. Commun. Heat Mass Transfer*, **32**, pp. 1057–1065.
- [14] Limtrakarn, W., Reepolmaha, S., and Dechaumphai, P., 2010, "Transient Temperature Distribution on the Corneal Endothelium During Ophthalmic Phacoemulsification: A Numerical Simulation Using the Nodeless Variable Element," *Asian Biomed.*, **4**(6), pp. 885–892.
- [15] Kumar, S., Acharya, S., Beuerman, R., and Palkama, A., 2006, "Numerical Solution of Ocular Fluid Dynamics in a Rabbit Eye: Parametric Effects," *Ann. Biomed. Eng.*, **34**, pp. 530–544.
- [16] Ooi, E., and Ng, E. Y. K., 2008, "Simulation of Aqueous Humor Hydrodynamics in Human Eye Heat Transfer," *Comput. Biol. Med.*, **38**, pp. 252–262.
- [17] Pennes, H. H., 1948, "Analysis of Tissue and Arterial Blood Temperatures in the Resting Human Forearm," *J. Appl. Physiol.*, **1**, pp. 93–122.
- [18] Pennes, H. H., 1998, "Analysis of Tissue and Arterial Blood Temperatures in the Resting Human Forearm," *J. Appl. Physiol.*, **85**(1), pp. 5–34.
- [19] Flyckt, V. M. M., Raaymakers, B. W., and Legendijk, J. J. W., 2006, "Modeling the Impact of Blood Flow on the Temperature Distribution in the Human Eye and the Orbit: Fixed Heat Transfer Coefficients Versus the Pennes Bioheat Model Versus Discrete Blood Vessels," *Phys. Med. Biol.*, **51**, pp. 5007–5021.
- [20] Ng, E. Y. K., and Ooi, E. H., 2006, "FEM Simulation of the Eye Structure With Bioheat Analysis," *Comput. Methods Programs Biomed.*, **82**, pp. 268–276.
- [21] Nakayama, A., and Kuwahara, F., 2008, "A General Bioheat Transfer Model Based on the Theory of Porous Media," *Int. J. Heat Mass Transfer*, **51**, pp. 3190–3199.
- [22] Mahjoob, S., and Vafai, K., 2009, "Analytical Characterization of Heat Transfer Through Biological Media Incorporating Hyperthermia Treatment," *Int. J. Heat Mass Transfer*, **52**, pp. 1608–1618.
- [23] Khanafer, K., and Vafai, K., 2009, Synthesis of Mathematical Models Representing Bioheat Transport (Advances in Numerical Heat Transfer), W. J. Min-kowycz and E. M. Sparrow, eds., Taylor & Francis, London, Vol. 3, pp. 1–28.
- [24] Shafahi, M., and Vafai, K., 2011, "Human Eye Response to Thermal Disturbances," *ASME Trans. J. Heat Transfer*, **133**, p. 011009.
- [25] Wessapan, T., Srisawatthisukul, S., and Rattanadecho, P., 2011, "Numerical Analysis of Specific Absorption Rate and Heat Transfer in the Human Body

- Exposed to Leakage Electromagnetic Field at 915 MHz and 2450 MHz,” *ASME Trans. J. Heat Transfer*, **133**, p. 051101.
- [26] Wessapan, T., Srisawatdhisukul, S., and Rattanadecho, P., 2011, “The Effects of Dielectric Shield on Specific Absorption Rate and Heat Transfer in the Human Body Exposed to Leakage Microwave Energy,” *Int. Commun. Heat Mass Transfer*, **38**, pp. 255–262.
- [27] Wessapan, T., Srisawatdhisukul, S., and Rattanadecho, P., 2012, “Specific Absorption Rate and Temperature Distributions in Human Head Subjected to Mobile Phone Radiation at Different Frequencies,” *Int. J. Heat Mass Transfer*, **55**, pp. 347–359.
- [28] Keangin, P., Wessapan, T., and Rattanadecho, P., 2011, “Analysis of Heat Transfer in Deformed Liver Cancer Modeling Treated Using a Microwave Coaxial Antenna,” *Appl. Therm. Eng.*, **32**, pp. 3243–3254.
- [29] Keangin, P., Rattanadecho, P., and Wessapan, T., 2011, “An Analysis of Heat Transfer in Liver Tissue during Microwave Ablation Using Single and Double Slot Antenna,” *Int. Commun. Heat Mass Transfer*, **38**, pp. 757–766.
- [30] Bernardi, P., Cavagnaro, M., Pisa, S., and Piazzi, E., 2000, “Specific Absorption Rate and Temperature Increases in the Head of a Cellular-Phone User,” *IEEE Trans. Microwave Theory Tech.*, **48**(7), pp. 1118–1126.
- [31] Park, S., Jeong, J., and Lim, Y., 2004, “Temperature Rise in the Human Head and Brain for Portable Handsets at 900 and 1800 MHz,” 4th International Conference on Microwave and Millimeter Wave Technology, ICMMT 2004, Beijing pp. 966–969.
- [32] Nakayama, A., and Kuwahara, F., 2008, “A General Bioheat Transfer Model Based on the Theory of Porous Media,” *Int. J. Heat Mass Transfer*, **51**, pp. 3190–3199.